



## Investigation of Carbon Dioxide Adsorption on Amino-Functionalized Mesoporous Silica

S. Salehi, M. Anbia\*

Research Laboratory of Nanoporous Materials, Faculty of Chemistry, Iran University of Science and Technology, Narmak, Tehran, Iran

### PAPER INFO

#### Paper history:

Received 25 December 2014  
Received in revised form 25 April 2015  
Accepted 30 April 2015

#### Keywords:

CO<sub>2</sub> Adsorption  
Mesoporous Silica  
SBA-3,  
Amine Functionalization  
Pentaethylenehexamine (PEHA).

### ABSTRACT

Carbon dioxide (CO<sub>2</sub>) adsorption on unfunctionalized and amino-functionalized SBA-3 materials are investigated and compared in this study. The synthesized materials are characterized by various techniques such as X-ray diffraction (XRD), Brunauer-Emmet-Teller (BET) method, Fourier transform infrared (FT-IR) and Scanning electron microscopy (SEM). The isotherms of these materials have been measured using volumetric method at 298 K up to 5 bar. The adsorption capacity of CO<sub>2</sub> by mesoporous silica was enhanced through functionalization with amine groups. It is observed that the pentaethylene hexamine functionalized SBA-3 (SBA-3/PEHA) possessed a higher adsorption capacity towards CO<sub>2</sub> than that of the other adsorbents.

doi: 10.5829/idosi.ije.2015.28.06c.04

## 1. INTRODUCTION

Carbon dioxide, most prevalent greenhouse gas usually formed via the combustion of fossil fuels, accumulates in the atmosphere, thus increase in the average global temperature and adverse effects of climatic change [1, 2]. Therefore, people are increasingly interested in controlling the concentration of CO<sub>2</sub> in the atmosphere by separating CO<sub>2</sub> from gas mixtures from major CO<sub>2</sub> emission sources [3-6]. Based on environmental and economical considerations, it is necessary to apply suitable and efficient technology for CO<sub>2</sub> separation with low energy consumption and operating cost. The conventional technologies for removal of CO<sub>2</sub> are cryogenic distillation, absorption, adsorption and membrane separation [7-9]. Among these technologies, adsorption using solid sorbents is known as one of the most efficient and affordable process due to low energy cost, greater capacity and selectivity, stable performance and easy operation [10-12]. The utilization of porous materials including activated carbons, zeolites, metal-organic frameworks (MOFs) and porous silicas (SBA-

15, MCM-48, etc.) as adsorptive materials for CO<sub>2</sub> capture has been well documented [13-18]. Mesoporous materials with an extremely high specific surface area and a uniform mesopore structure were extensively studied in the past decade [19, 20] due to have high potentials in the application fields of catalysis and adsorption. Highly ordered mesoporous molecular sieves including M41S and SBA typed materials have attracted increasing attention since their first report by Mobil oil researchers [21]. SBA-type silica materials are ordered mesoporous materials with higher hydrothermal stability than MCM-41. Furthermore, the microporosity in SBA-3 was considerably larger than those in SBA-15 [22, 23]. SBA-3-type mesoporous molecular sieves were synthesized using a low molecular weight alkyl quaternary ammonium template room temperature and under acidic condition. Thermal and mechanical properties of SBA-3 are critical features for their application as adsorbent [24], leading modified SBA-3 widely used in adsorption fields. Amine- functionalized mesoporous silicas for CO<sub>2</sub> adsorption are getting great attention because of their efficient adsorption performance, rapid mass transfer kinetics and simplicity of cyclic regeneration under mild conditions [25].

\*Corresponding Author's Email: [anbia@iust.ac.ir](mailto:anbia@iust.ac.ir) (M. Anbia)

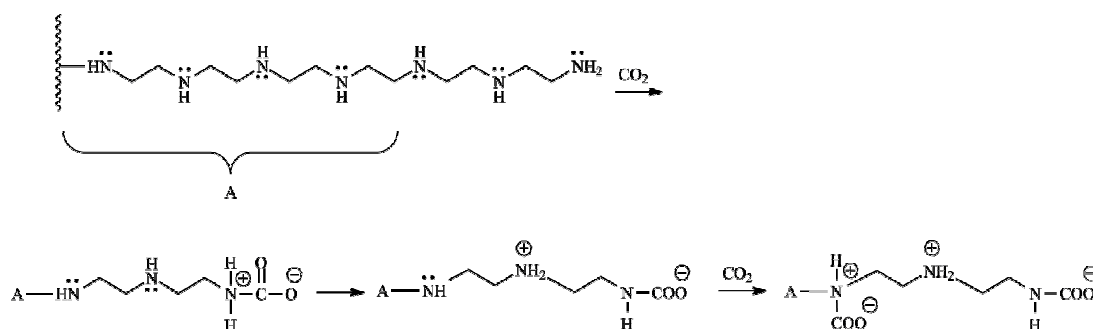


Figure 1. Reactions between  $\text{CO}_2$  and SBA-3/PEHA.

In general, the functionalization of the surface of the mesopores has been achieved by amine-impregnated and amine-grafted materials via weak interactions and strong covalent bonding, respectively [26]. Typically, the amine-grafted adsorbents exhibit comparatively higher stability in cyclic runs and higher adsorption rate than the amine-impregnated ones.

In this study, various amine functional groups have been studied for functionalization of the SBA-3 to enhance  $\text{CO}_2$  adsorption, in view of the high affinity and interaction between the amine groups and acidic gas. These functionalized materials are prepared by post-synthesis grafting method. After characterization of these materials by X-ray diffraction (XRD), Brunauer–Emmet–Teller (BET), Fourier transform infrared (FT-IR) and Scanning electron microscopy (SEM) analysis,  $\text{CO}_2$  adsorption capacity have been measured by volumetric measurements at 298 K up to 5 bar.

## 2. EXPERIMENTAL

### 2. 1. Synthesis of SBA-3

The preparation procedure was taken from the literature [27]. The SBA-3 samples were synthesized using tetraethyl orthosilicate (TEOS, Merck) as the silica source and cetyltrimethylammonium bromide (CTAB, Merck) as template.

In a typical synthesis, 1 g of CTAB was dissolved in 47 mL of deionized water and acidified with 15 mL of HCl to obtain clear solution. TEOS (4.45 mL) was then added dropwise to the acidic CTAB solution stirring at 400 rpm at 30 °C, then the solution was left for 1 h. A white precipitate was recovered by filtration and washed with deionized water and dried at 100°C overnight. Subsequently, the surfactant was removed by calcination at 550°C in air for 5 h, increasing the temperature to 550°C at 1 °C/min of the heating rate.

### 2. 2. Synthesis of SBA-3 Functionalized with APTES

2 g of 3-aminopropyl trimethoxysilane (APTES, Merck) was mixed with 2 g of SBA-3 in 60 mL of anhydrous toluene (for 10 h under reflux

conditions and a nitrogen atmosphere). The resulting precipitate was filtered, washed with dichloromethane and ethanol, and was dried. It was then extracted with a soxhlet setup with a mixture of dichloromethane and ethanol with the ratio of 1:1 (V/V) to remove the remaining silylating reagent and was then vacuum-dried at 70 °C, overnight. The product obtained was denoted as SBA-3/APTES.

### 2. 3. Synthesis of SBA-3 Functionalized with PEHA

1 g of pentaethylene hexamine (PEHA, Merck) was dissolved in 50 g ethanol under stirring for 40 min at room temperature, and then 2 g SBA-3 was added. After refluxing for 4 h, the resulting mixture was evaporated at 80 °C. Finally, the samples were dried in air for 1 h at 100°C and denoted as SBA-3/PEHA (Figure 1).

### 2. 4. Synthesis of SBA-3 Functionalized with EDA

For the preparation of SBA-3/EDA, a similar process to that of the SBA-3/PEHA was used and PEHA was replaced by ethylenediamine (EDA, Merck).

### 2. 5. Characterization

The porosity characteristics of the mesoporous silica sorbents were determined by  $\text{N}_2$  adsorption–desorption experiments performed at 77 K on micromeritics model ASAP 2010 sorptometer. The specific surface area ( $S_{\text{BET}}$ ) was determined from the linear part of the Brunauer–Emmet–Teller (BET) equation. Pore size distribution was estimated from the adsorption branch of the isotherm by the Barrett–Joyner–Halenda (BJH) method. The Fourier transform infrared spectra for the unfunctionalized and functionalized silica materials were measured on a DIGILAB FTS 7000 instrument under attenuated total reflection (ATR) mode using a diamond module. X-ray diffraction (XRD) was used to identify the crystal phases of the mesoporous silica materials. The XRD patterns were recorded with a Philips 1830 powder X-ray diffractometer using Cu-K $\alpha$  radiation source of wavelength 1.5406 for  $2\theta$  ranging from 1° to 10° with a 2 $\theta$  step size of 0. scanning 018° and a step time of 1 s.

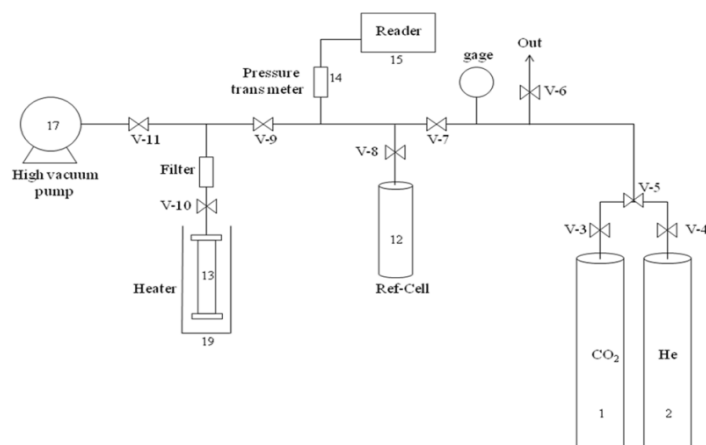


Figure 2. Setup for sorption/desorption capacity test.

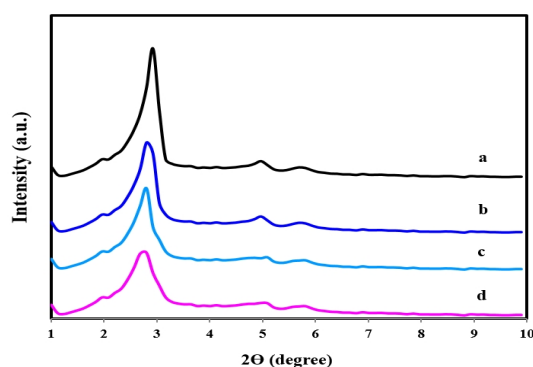


Figure 3. XRD patterns of SBA-3 (a), SBA-3/EDA (b), SBA-3/APTES (c) and SBA-3/PEHA (d).

The surface features and morphology of the materials were investigated by using electron microscopy (SEM PHILIPS XL30). The samples were coated with gold in order to increase their conductivity before scanning.

**2. 6. CO<sub>2</sub> Adsorption Measurement** The carbon dioxide capacity of the synthesized materials was evaluated using volumetric method by setup shown in Figure 2. The volumetric method for carbon dioxide uptake measurements is extensively adopted because of its simplicity, low-cost, and easy assemblage. 1 g of sample was loaded inside the sample cell (13) and attached to the system. Then the system was carefully checked with the inert Helium gas flow to ensure all connections have no leakage. The existing gas inside the system was swept out with Helium.

Afterwards, to remove residual solvents trapped in nanopores during synthesis, all the valves except 11, 10, 9 and 8 were closed and the system was vacuumed and heated at 473 K for 1.5 h. Ultra-high purity carbon

dioxide (99.999%) was introduced into adsorption unit for the CO<sub>2</sub> adsorption measurements. To perform an adsorption test, the valve of the CO<sub>2</sub> cylinder was opened and the CO<sub>2</sub> pressure was regulated at the desired value, then valves 7 and 8 were opened to reach a pressure balance in the reference cell (12).

Afterwards, valve 10 was immediately opened and the pressure decrease was recorded. The pressure of adsorption cell decreased due to some dead volume and some CO<sub>2</sub> adsorption. The portion of dead volume was calculated via helium tests and subtracted from the total pressure change. Finally, the exact pressure decrease resulting from CO<sub>2</sub> adsorption could be calculated.

### 3. RESULTS AND DISCUSSION

**3. 1. Characterization of the Adsorbent** X-ray diffractograms for SBA-3 as well as functionalized silica materials are presented in Figure 3. The XRD patterns display three peaks at  $2\theta = 2.76^\circ$ ,  $4.74^\circ$  and  $5.30^\circ$  respectively. These peaks were indexed as (100), (110) and (200) crystal facets, which belong to one-dimensional hexagonal (P6m) mesostructures. It must be noted that the amino-functionalized SBA-3 materials maintained the three peaks (at  $d$  spacing 100, 110 and 200) of the XRD pattern with reduced intensity compared with that for SBA-3. The intensity decrease of diffraction peaks indicates the lowering of mesopore uniformity. Moreover, the XRD patterns of SBA-3 materials demonstrate that hexagonally ordered structure of SBA-3 was persistent after the functionalization.

N<sub>2</sub> adsorption-desorption isotherms of unfunctionalized and amino-functionalized SBA-3 materials are presented in Figure 4. SBA-3 materials show three distinct regions of N<sub>2</sub> adsorption isotherms. The initial part of the isotherm indicates a high ‘knee’,

followed by a slower growth in the adsorbed volume at low relative pressures ( $>0.1 P/P_0$ ), may be attributed to a monolayer-multilayer adsorption on the pore walls. The high “knee” may illustrate the presence of the micropores inside SBA-3. At a relative pressure  $P/P_0$  between 0.2 and 0.3, the isotherm exhibits a sharp step characteristic of capillary condensation within the mesopores. These isotherms show no hysteresis loop between adsorption and desorption branches, similar to that reported in the literature [28]. A very slow linear increase at higher relative pressures ( $>0.3 P/P_0$ ) shows the adsorption on the outer surface of SBA-3.

**TABLE 1.** Textural properties determined from nitrogen adsorption-desorption experiments at 77 K.

Adsorbent	$A_{\text{BET}}$ ( $\text{m}^2 \text{g}^{-1}$ )	Average pore size ( $\text{\AA}$ )	$V_p$ ( $\text{cm}^3 \text{g}^{-1}$ )
SBA-3	1435	21.6	0.96
SBA-3/EDA	1290	19.2	0.82
SBA-3/APTES	1092	16.8	0.67
SBA-3/PEHA	1005	16.3	0.62

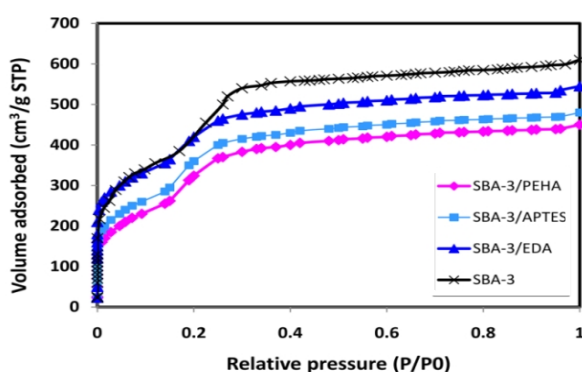


**Figure 4.** Adsorption-desorption isotherms of nitrogen at 77 K on SBA-3, SBA-3/EDA, SBA-3/APTES and SBA-3/PEHA.

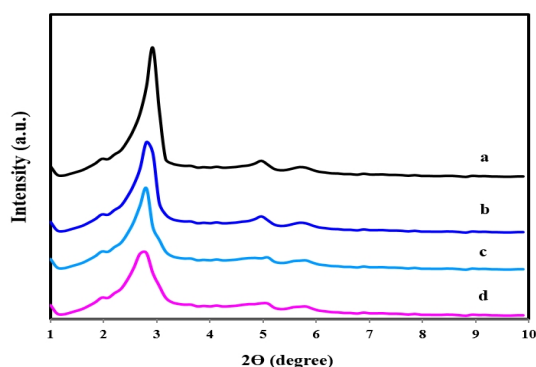


**Figure 3.** XRD patterns of SBA-3 (a), SBA-3/EDA (b), SBA-3/APTES (c) and SBA-3/PEHA (d).

The overview features of these isotherms can be explained as the superposition of type I (for micropore) and type IV (for mesopore) isotherms [29, 30].

The Brunauer-Emmett-Teller (BET) surface area, pore volumes and average pore diameter for each sample are listed in Table 1. The pure silica sample displayed much higher BET surface area, average pore diameter and pore volume when compared to the amino-functionalized SBA-3 materials. Introduction of amino functional groups into SBA-3 structure resulted in decrease of textural parameters.

Qualitative identification of functional groups was accomplished by FT-IR spectroscopy. Figure 5 shows the FT-IR spectrum of prepared adsorbents over the range of  $4000\text{--}400 \text{ cm}^{-1}$ . A broad band in the range of  $3700\text{--}3010 \text{ cm}^{-1}$  is seen which can be attributed to the framework of Si-OH group interaction with the defect sites and adsorbed water molecules. The Si-OH peak appears at about  $3460 \text{ cm}^{-1}$ , while peaks for the weak single Si-OH groups derived from the germinal Si-OH groups were observed at  $3740 \text{ cm}^{-1}$ . The asymmetric stretching vibrations of Si-O-Si and Si-OH are observed by the absorption bands at  $1000\text{--}1360 \text{ cm}^{-1}$  and the band at  $790 \text{ cm}^{-1}$  is assigned to free silica. In general, the functionalized silicas with amino groups show a broad  $\text{NH}_2$  stretching at  $3250\text{--}3450 \text{ cm}^{-1}$ , an N-H deformation peak at  $1640\text{--}1560 \text{ cm}^{-1}$ , C-H stretching of methyl groups at  $3000\text{--}2850$  and  $1450 \text{ cm}^{-1}$ . The symmetric and asymmetric stretching vibrations of the  $-\text{NH}_2$  groups appear at  $3250\text{--}3450 \text{ cm}^{-1}$  but in the spectrum of amino-functionalized SBA-3 materials are probably masked by the broad peak due to adsorbed water molecules [31]. In addition, in comparison with the SBA-3/PEHA, the amino bands are weaker for SBA-3/APTES and SBA-3/EDA.

Scanning electron microscopy (SEM) images of as-synthesized samples are shown in Figure 6. It can be seen that the well regular shape and morphology are the same in all of unfunctionalized and functionalized silica materials. This suggests the shape of particles is not changed and morphology of amino-functionalized SBA-3 materials have remained intact after functionalization.

The adsorption isotherms of  $\text{CO}_2$  on unfunctionalized and amino-functionalized SBA-3 materials at ambient temperature (298 K) and different pressures in the range of 0–5 bar are shown in Figure 7. The experimental result indicates that the curvature of isotherm adsorption equilibrium belongs to type I and follows by kinetic Langmuir model [32].

The steep slope of the Type I curve in Figure 7 where it is linear at low pressures would reflect a monomolecular layer of adsorbate on the solid surface according to Langmuir's model and assumptions [33]. The isotherm of SBA-3/PEHA, SBA-3/APTES and SBA-3/EDA shows a step increase at low pressure (below 1 bar) followed by a constant increase.



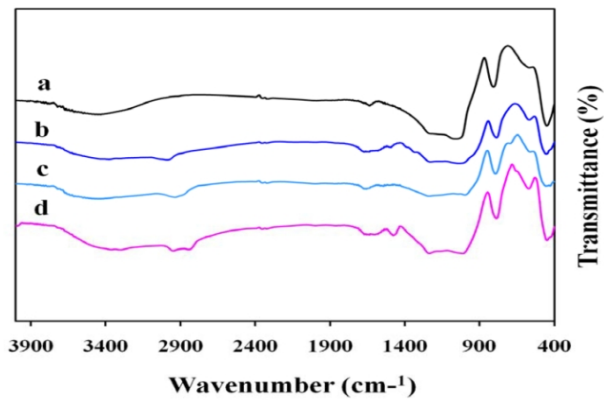


**Figure 5.** FT-IR spectra of SBA-3 (a), SBA-3/EDA (b), SBA-3/APTES (c) and SBA-3/PEHA (d).

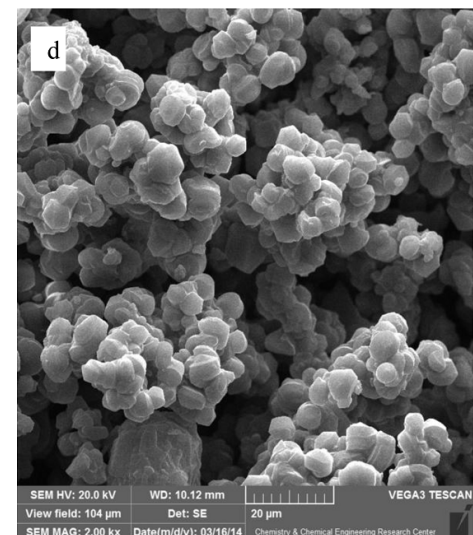
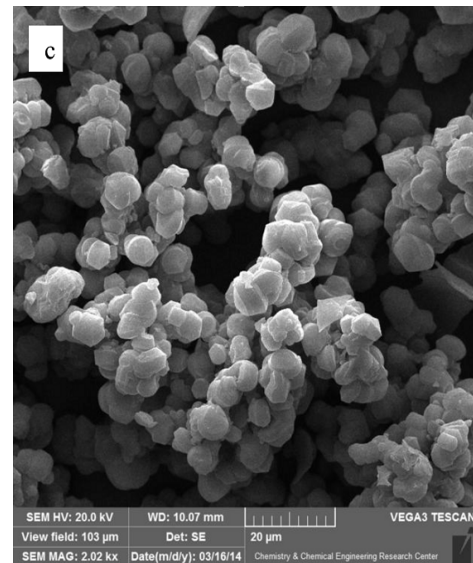
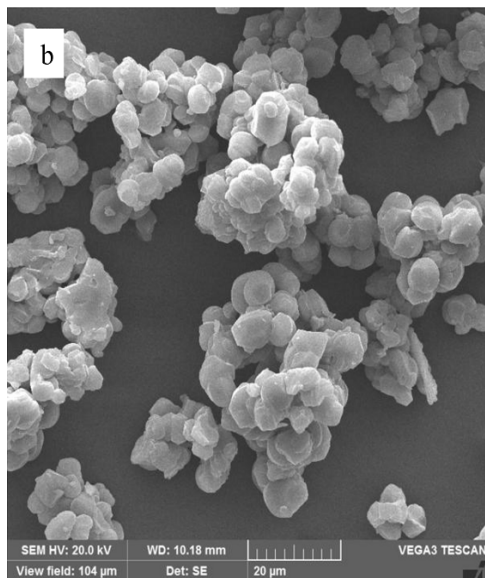
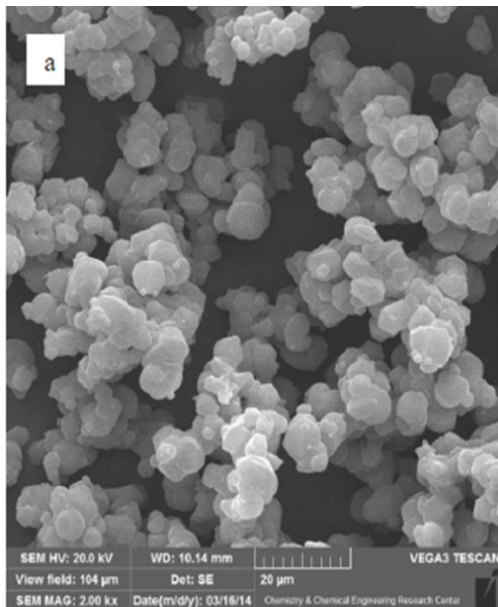


**Figure 6.** SEM images of SBA-3 (a), SBA-3/EDA (b), SBA-3/APTES (c) and SBA-3/PEHA (d).

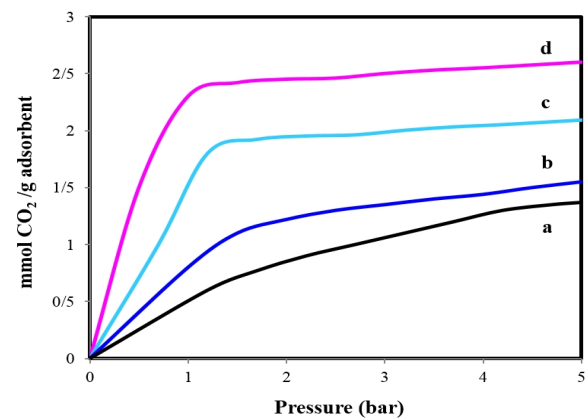


**Figure 7.** CO<sub>2</sub> adsorption capacity of SBA-3 (a), SBA-3/EDA (b), SBA-3/APTES (c) and SBA-3/PEHA (d) at different pressures and 298 K.

It is clear from the figure that at pressure 1 bar and 298 K, SBA-3/PEHA shows the highest CO<sub>2</sub> adsorption capacity. Pure silica surface does not provide strong adsorption sites to interact strongly with CO<sub>2</sub> due to the fact that the hydroxyl groups on the silica surface fail to induce strong interactions with CO<sub>2</sub>. The adsorption capacity of CO<sub>2</sub> by mesoporous silica was enhanced through functionalization with amine groups. The enhancement in CO<sub>2</sub> adsorption over functionalization of SBA-3 with amine groups is due to acid-base interaction between basic amine groups and acidic CO<sub>2</sub>. Generally, active alkali -NH<sub>2</sub> group possess lone a pair of electrons on N atom which undergoes nucleophilic attack on the C atom of acidic CO<sub>2</sub>, leading to formation of carbamate through carboxyl group. The active H atom in carboxyl group can then form ion pairs through hydrogen bond with the nearby amine group, and hence stabilizes the chemisorption of CO<sub>2</sub> [34, 35]. However, stabilization of carbamate in the course of hydrogen bonding decreases the number of free amine groups. Thus, one mole CO<sub>2</sub> stabilization requires two moles of amine groups (Figure 1).

The CO<sub>2</sub> adsorption capacity increases with increase in amine number of the functionalized mesoporous silica where primary amine and secondary amine are involved in CO<sub>2</sub> adsorption with similar efficiency [36]. SBA-3/PEHA can offer a great number of adsorption sites due to high number of amine groups on the surface of the SBA-3/PEHA.

#### 4. CONCLUSIONS

SBA-3 as well as functionalized silica materials SBA-3 materials have been successfully synthesized and characterized by XRD, BET, FT-IR and SEM analysis. The pure silica sample displayed much higher BET surface area, average pore diameter and pore volume when compared to the amino-functionalized SBA-3 materials. This phenomenon suggests the introduction of amino functional groups into SBA-3 structure resulted in decrease of textural parameters. The adsorption capacity of CO<sub>2</sub> by mesoporous silica was enhanced through interaction between the amine groups and acidic gas. According to the results, A significant enhancement in the carbon dioxide adsorption capacity was observed in the SBA-3/PEHA. CO<sub>2</sub> adsorption capacity was measured by volumetric measurements at 298 K up to 5 bar.

#### 5. REFERENCES

1. Anson, A., Lin, C.C., Kuznicki, S.M. and Sawada, J.A., "Adsorption of carbon dioxide, ethane, and methane on titanosilicate type molecular sieves", *Chemical Engineering Science*, Vol. 64, No. 16, (2009), 3683-3687.
2. An, H., Feng, B. and Su, S., "Co 2 capture by electrothermal swing adsorption with activated carbon fibre materials", *International Journal of Greenhouse Gas Control*, Vol. 5, No. 1, (2011), 16-25.
3. Zhao, G., Aziz, B. and Hedin, N., "Carbon dioxide adsorption on mesoporous silica surfaces containing amine-like motifs", *Applied Energy*, Vol. 87, No. 9, (2010), 2907-2913.
4. Zhao, L., Sang, L., Chen, J., Ji, J. and Teng, H.H., "Aqueous carbonation of natural brucite: Relevance to co2 sequestration", *Environmental Science & Technology*, Vol. 44, No. 1, (2009), 406-411.
5. Mignardi, S., De Vito, C., Ferrini, V. and Martin, R., "The efficiency of co 2 sequestration via carbonate mineralization with simulated wastewaters of high salinity", *Journal of Hazardous Materials*, Vol. 191, No. 1, (2011), 49-55.
6. Zevenhoven, R., Fagerlund, J. and Songok, J.K., "Co2 mineral sequestration: Developments toward large-scale application", *Greenhouse Gases: Science and Technology*, Vol. 1, No. 1, (2011), 48-57.
7. Olajire, A.A., "Co 2 capture and separation technologies for end-of-pipe applications—a review", *Energy*, Vol. 35, No. 6, (2010), 2610-2628.
8. Samanta, A., Zhao, A., Shimizu, G.K., Sarkar, P. and Gupta, R., "Post-combustion co2 capture using solid sorbents: A review", *Industrial & Engineering Chemistry Research*, Vol. 51, No. 4, (2011), 1438-1463.
9. Rhodes, J.S. and Keith, D.W., "Engineering economic analysis of biomass igcc with carbon capture and storage", *Biomass and Bioenergy*, Vol. 29, No. 6, (2005), 440-450.
10. Aronu, U.E., Svendsen, H.F. and Hoff, K.A., "Investigation of amine amino acid salts for carbon dioxide absorption", *International Journal of Greenhouse Gas Control*, Vol. 4, No. 5, (2010), 771-775.
11. Gray, M., Soong, Y., Champagne, K., Baltrus, J., Stevens, R., Toochinda, P. and Chuang, S., "Co 2 capture by amine-enriched fly ash carbon sorbents", *Separation and Purification Technology*, Vol. 35, No. 1, (2004), 31-36.
12. Jang, H.T., Park, Y., Ko, Y.S., Lee, J.Y. and Margandan, B., "Highly siliceous mcm-48 from rice husk ash for co 2 adsorption", *International Journal of Greenhouse Gas Control*, Vol. 3, No. 5, (2009), 545-549.
13. Anbia, M., Hoseini, V. and Mandegarzarad, S., "Synthesis and characterization of nanocomposite mcm-48-peha-dea and its application as co2 adsorbent", *Korean Journal of Chemical Engineering*, Vol. 29, No. 12, (2012), 1776-1781.
14. Anbia, M. and Hoseini, V., "Enhancement of co 2 adsorption on nanoporous chromium terephthalate (mil-101) by amine modification", *Journal of Natural Gas Chemistry*, Vol. 21, No. 3, (2012), 339-343.
15. Kamarudin, K.S.N. and Alias, N., "Adsorption performance of mcm-41 impregnated with amine for co 2 removal", *Fuel Processing Technology*, Vol. 106, (2013), 332-337.
16. Taghipoura, Z., Eisazadeh, H. and Tanzifi, M., "Modification of polyaniline/polystyrene and polyaniline/metal oxide structure by surfactant", *International Journal of Engineering-Transactions B: Applications*, Vol. 27, No. 2, (2013), 227.
17. Wu, X., Yuan, B., Bao, Z. and Deng, S., "Adsorption of carbon dioxide, methane and nitrogen on an ultramicroporous copper metal-organic framework", *Journal of Colloid and Interface Science*, Vol. 430, No., (2014), 78-84.
18. McEwen, J., Hayman, J.-D. and Yazaydin, A.O., "A comparative study of co 2, ch 4 and n 2 adsorption in zif-8, zeolite-13x and bpl activated carbon", *Chemical Physics*, Vol. 412, No., (2013), 72-76.

19. Anbia, M. and Davijani, A., "Synthesis of ethylenediamine-modified ordered mesoporous carbon as a new nanoporous adsorbent for removal of cu (ii) and pb (ii) ions from aqueous media", *International Journal of Engineering-Transactions C: Aspects*, Vol. 27, No. 9, (2014), 1415-1423.
20. Anbia, M. and Ghaffari, A., "Modified nanoporous carbon material for anionic dye removal from aqueous solution", *International Journal of Engineering-Transactions B: Applications*, Vol. 25, No. 4, (2012), 259-270.
21. Zhao, D., Huo, Q., Feng, J., Chmelka, B.F. and Stucky, G.D., "Nonionic triblock and star diblock copolymer and oligomeric surfactant syntheses of highly ordered, hydrothermally stable, mesoporous silica structures", *Journal of the American Chemical Society*, Vol. 120, No. 24, (1998), 6024-6036.
22. Albouy, P.-A. and Ayrat, A., "Coupling x-ray scattering and nitrogen adsorption: An interesting approach for the characterization of ordered mesoporous materials. Application to hexagonal silica", *Chemistry of Materials*, Vol. 14, No. 8, (2002), 3391-3397.
23. Ryoo, R., Ko, C.H., Kruk, M., Antochshuk, V. and Jaroniec, M., "Block-copolymer-templated ordered mesoporous silica: Array of uniform mesopores or mesopore-micropore network?", *The Journal of Physical Chemistry B*, Vol. 104, No. 48, (2000), 11465-11471.
24. Galarneau, A., Desplandier-Giscard, D., Di Renzo, F. and Fajula, F., "Thermal and mechanical stability of micelle-templated silica supports for catalysis", *Catalysis Today*, Vol. 68, No. 1, (2001), 191-200.
25. Liu, X., Zhou, L., Fu, X., Sun, Y., Su, W. and Zhou, Y., "Adsorption and regeneration study of the mesoporous adsorbent sba-15 adapted to the capture/separation of co<sub>2</sub> and ch<sub>4</sub>", *Chemical Engineering Science*, Vol. 62, No. 4, (2007), 1101-1110.
26. Sayari, A., Belmabkhout, Y. and Serna-Guerrero, R., "Flue gas treatment via co<sub>2</sub> adsorption", *Chemical Engineering Journal*, Vol. 171, No. 3, (2011), 760-774.
27. Huo, Q., Margolese, D.I. and Stucky, G.D., "Surfactant control of phases in the synthesis of mesoporous silica-based materials", *Chemistry of Materials*, Vol. 8, No. 5, (1996), 1147-1160.
28. Nowińska, K., Formaniak, R., Kaleta, W. and Waclaw, A., "Heteropoly compounds incorporated into mesoporous material structure", *Applied Catalysis A: General*, Vol. 256, No. 1, (2003), 115-123.
29. Göltner, C.G., Smarsly, B., Berton, B. and Antonietti, M., "On the microporous nature of mesoporous molecular sieves", *Chemistry of Materials*, Vol. 13, No. 5, (2001), 1617-1624.
30. Selvam, P., Bhatia, S.K. and Sonwane, C.G., "Recent advances in processing and characterization of periodic mesoporous mcm-41 silicate molecular sieves", *Industrial & Engineering Chemistry Research*, Vol. 40, No. 15, (2001), 3237-3261.
31. Jaroniec, C., Kruk, M., Jaroniec, M. and Sayari, A., "Tailoring surface and structural properties of mcm-41 silicas by bonding organosilanes", *The Journal of Physical Chemistry B*, Vol. 102, No. 28, (1998), 5503-5510.
32. Bao, Z., Yu, L., Ren, Q., Lu, X. and Deng, S., "Adsorption of co<sub>2</sub> and ch<sub>4</sub> on a magnesium-based metal organic framework", *Journal of Colloid and Interface Science*, Vol. 353, No. 2, (2011), 549-556.
33. Bao, Z., Alnemrat, S., Yu, L., Vasiliev, I., Ren, Q., Lu, X. and Deng, S., "Kinetic separation of carbon dioxide and methane on a copper metal-organic framework", *Journal of Colloid and Interface Science*, Vol. 357, No. 2, (2011), 504-509.
34. Yue, M.B., Sun, L.B., Cao, Y., Wang, Z.J., Wang, Y., Yu, Q. and Zhu, J.H., "Promoting the co<sub>2</sub> adsorption in the amine-containing sba-15 by hydroxyl group", *Microporous and Mesoporous Materials*, Vol. 114, No. 1, (2008), 74-81.
35. Zhao, H., Hu, J., Wang, J., Zhou, L. and Liu, H., "Co<sub>2</sub> capture by the amine-modified mesoporous materials", *Acta Physico-Chimica Sinica*, Vol. 23, No. 6, (2007), 801-806.
36. Hiyoshi, N., Yogo, K. and Yashima, T., "Adsorption of carbon dioxide on modified mesoporous materials in the presence of water vapor", *Studies in Surface Science and Catalysis*, Vol. 154, No., (2004), 2995-3002.

## Investigation of Carbon Dioxide Adsorption on Amino-Functionalized Mesoporous Silica

S. Salehi, M. Anbia

Research Laboratory of Nanoporous Materials, Faculty of Chemistry, Iran University of Science and Technology, Narmak, Tehran, Iran

### PAPER INFO

چکیده

#### Paper history:

Received 25 December 2014  
Received in revised form 25 April 2015  
Accepted 30 April 2015

#### Keywords:

CO<sub>2</sub> Adsorption  
Mesoporous Silica  
SBA-3,  
Amine Functionalization  
Pentaethylenehexamine (PEHA).

جاذبه‌های SBA-3 عامل دار نشده و عامل دار شده با گروه‌های آمینی، برای جذب CO<sub>2</sub> سنتز گردید. ویژگی‌های ساختاری و فیزیکی جاذب‌های سنتز شده با روش‌های پراش اشعه ایکس (XRD)، آنالیز جذب و واجذب نیتروژن، اسپکتروسکوپی مادون قرمز تبدیل فوریه (FTIR) و میکروسکوپی الکترونی روبشی (SEM) شناسایی شده است. مقدار گاز ذخیره شده در دمای محیط (۲۹۸ K) و فشار گاز تا ۵ bar به روش حجم سنجی اندازه‌گیری شده است. از طریق عامل دار کردن مزومتخلخل سیلیکاتی با گروه‌های آمینی، ظرفیت جذب CO<sub>2</sub> افزایش می‌یابد. جاذب SBA-3/PEHA بیشترین میزان ظرفیت جذب CO<sub>2</sub> را نسبت به دیگر جاذب‌ها از خود نشان می‌دهد.

doi: 10.5829/idosi.ije.2015.28.06c.04